

Nanoseismicity forecasts sinkhole collapse in the Dead Sea coast years before their final collapse

Meir Abelson¹, Tatiana Aksinenko², Ittai Kurzon¹, Vladimir Pinsky², Gidon Baer¹, Ran Nof^{1,2}, and Yoseph Yechieli^{1,3}

¹*Geological Survey of Israel, Jerusalem 95501, Israel*

²*Geophysical Institute of Israel, Lod 71100, Israel*

³*Zuckerberg Center, Ben-Gurion University of the Negev, Sde Boker 8499000, Israel*

The seismic monitoring system used in this study was built by the Institute of Mine Seismology (IMS) for detection of rockmass stability overlying deep mines (Mendecki, 1997). Five geophones were planted in five boreholes at various depths. The boreholes were drilled in the alluvial fan around the Mineral Beach sinkhole cluster. Five 14 Hz tri-axial geophones (frequency range 9-2000 Hz) were buried within five boreholes, at distances of several hundred meters apart (see details in Fig. DR1). In order to locate the hypocenter depths, the geophones were positioned at various depths, with the deepest (25 m deep) in the lowest station in the east (Seismic Station #1, altitude -427 m.b.s.l), and the shallowest (10 m deep) in Seismic Station #5 in the west (-399 m.b.s.l.) (Fig. DR1). The geophones were attached to the borehole pipe by concrete for improved reception of the seismic signal. The data from the data logger, with sampling rate of 3000 sps, were transmitted by omnidirectional antenna (Fig. DR1) to the Geophysical Institute of Israel for processing. The locations of the seismic events were calculated by fitting the observed arrival times of P and S waves (Fig. DR2) and by a velocity model of the study area. The velocity model was built from two crosscutting seismic refraction profiles (Shtivelman, 1998; Ezersky, 2010), and from boreholes by downhole velocity measurements (Shtivelman, 2003). The salt layer top is in a depth of 35-40 m with a seismic velocity around 3000 m/s. During the seismic survey between June 28 and September 7, 2012, 82 events were recorded. Seven (7) distant events ($-1.5 \leq M_L \leq 0.4$) were located several kilometers away from Mineral Beach, and related to events from tectonic origin (Fig. DR3). The rest 75 nanoseismic events ($-3 \leq M_L \leq -2$) were recorded around the sinkholes, and related to concealed activity of sediments instabilities above cavities.

Interferometric Synthetic Aperture Radar (InSAR) measurements show the phase differences (translated to satellite to ground line of sight surface deformation) that occurred between any two chosen acquisition dates (Fig. 4). Atmospheric effects, which are common artifacts in this technique, are of different scale and pattern than the localized and linear sinkhole-related deformation and are thus of less concern in terms of obscuring the signal at the scale of the sinkhole-related deformation.

The shortcomings of the seismic monitoring relative to the InSAR are its expenditure and complicated operations, especially due to drillings. The accuracy of the hypocenter depth is highly dependent on the gradients of geophone depths (depth difference to spacing between geophones). Therefore, higher accuracy in hypocenter depths demands deeper boreholes, which makes the seismic monitoring much more expensive. Secondly, the 2-months seismic monitoring is a snapshot of the subsurface deformation relative to the several-years process of sinkhole appearance on the surface. Therefore, at such initial stage of sinkhole appearance in the ‘nanoseismic cloud’ (Fig. DR1), the epicenters locations are not necessarily correlate with the location of individual sinkholes as usually obtained by the InSAR (e.g., Nof et al., 2013); it merely defines the zone that is prone to sinkhole collapses in the following years. In order to record seismicity of a single sinkhole (i.e., correlation between epicenters location and individual sinkholes), a much longer monitoring, i.e., much more nanoseismic events, is required.

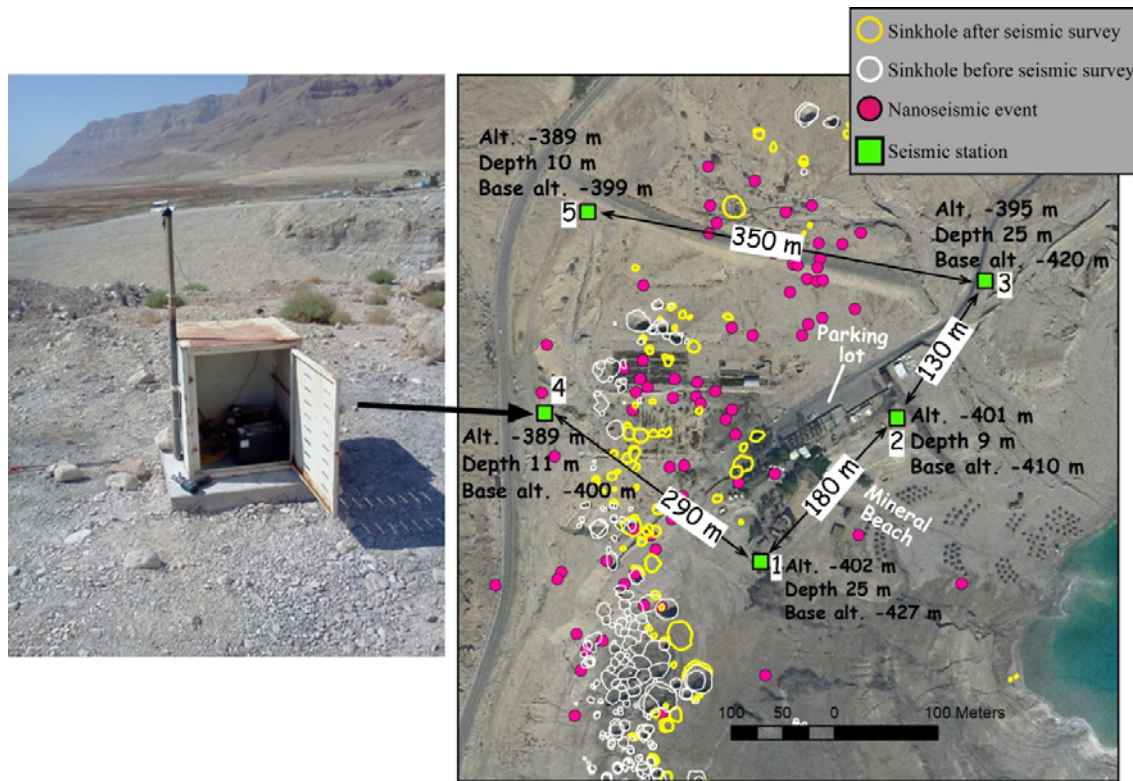


Figure DR1. Location, altitude and depth of seismic stations relative to sinkholes that occurred before and after the seismic survey in 2012. Base and top elevations of borehole, where geophones were planted, are marked near each seismic station, as well as the distances between adjacent boreholes. The photograph on the left displays a seismic station with its data logger and GPS antenna. Note the new sinkholes that appeared in the spa and its margins (shown by yellow circles at the SW side of the parking lot) in 2014-2016, after the seismic survey.

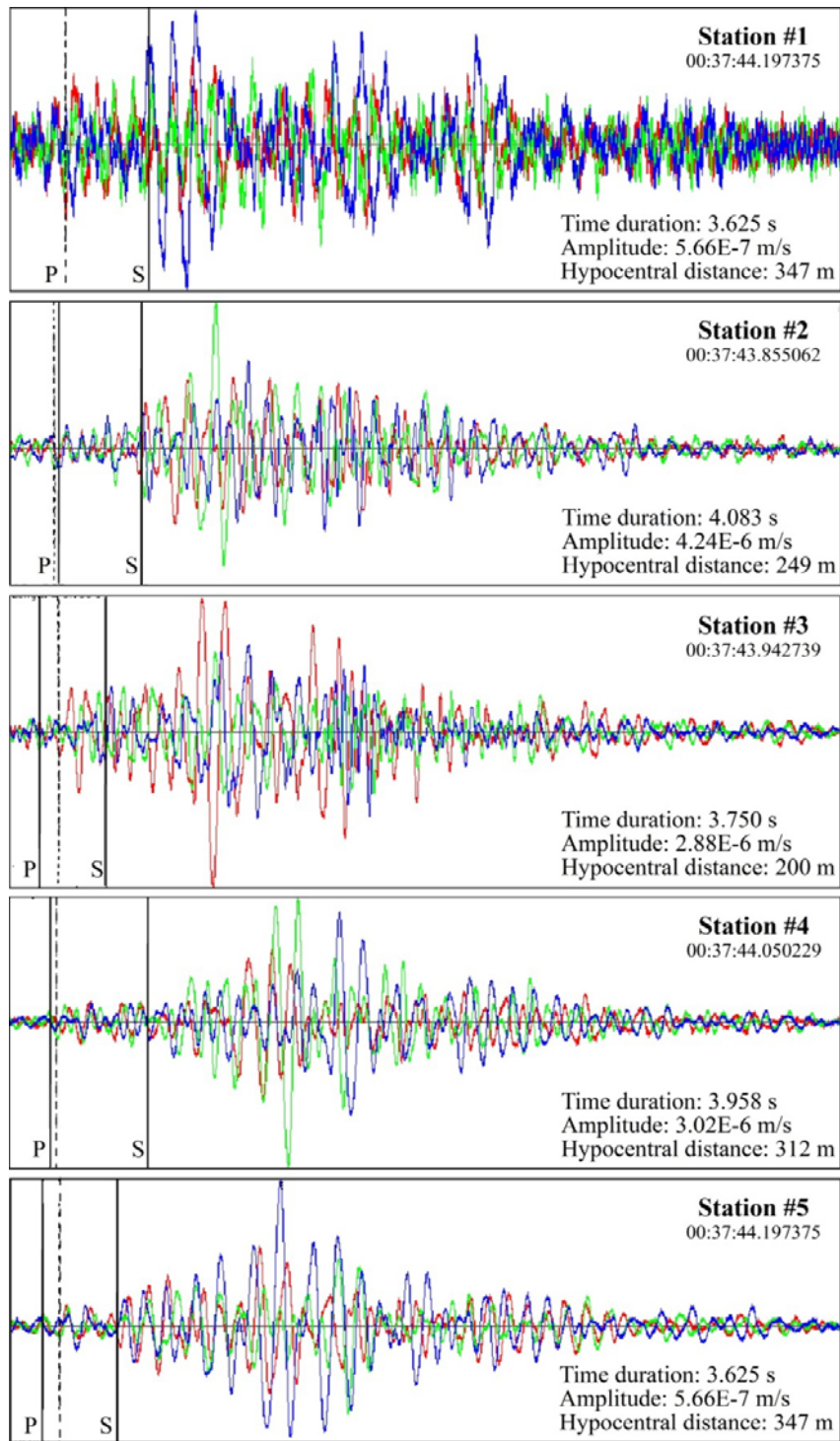


Figure DR 2. Examples of waveforms of event on 25/8/2012 (00:37:43). P and S arrivals are marked for each station.

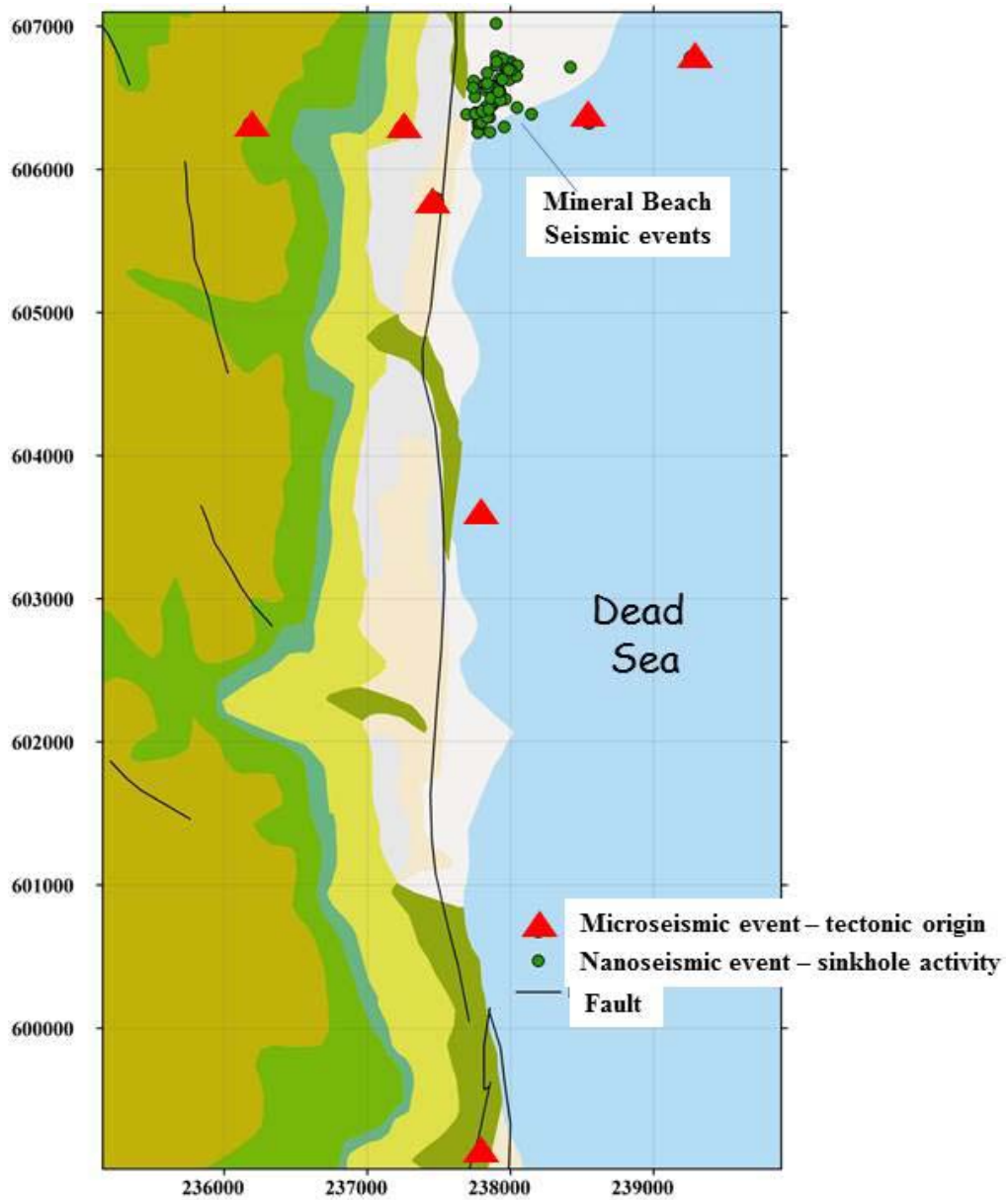


Figure DR 3. Epicenters of seismic events are marked on a geological map around Mineral Beach (Sneh et al., 1998): seven remote events, $-1.5 < M_L < 0.4$ (red triangles), possibly of tectonic origin, and 75 nanoseismic events due to instabilities above cavities (green points). Brown-green provinces are Cretaceous rocks of the Dead Sea rift walls, and light colors are top of Holocene sediments filling the Dead Sea rift.

References

- Ezersky, M., 2010, Improvement of the seismic refraction method for mapping of the buried salt layers along the Dead Sea shoreline: Geophysical Institute of Israel Report MNI-ES-1-2010, 36 pp.

- Mendecki, A. J. (Ed.), 1997, Seismic Monitoring in Mines, 1 ed., 262 pp., Chapman & Hall.
- Nof, R., Baer, G., Ziv, A., Eyal, Y., Raz, E., Atzori, S., and Salvi, S., 2013, Sinkhole precursors along the Dead Sea, Israel, revealed by SAR interferometry: Geology, v. 41, p. 1019–1022, doi:10.1130/G34505.1.
- Shtivelman, V., 1998, Shallow seismic surveys in the sinkhole areas along the Dead Sea coast: Geophysical Institute of Israel, Report No 837/85/98.
- Shtivelman, V., 2003, Downhole and refraction seismic surveys at three sinkhole sites on the Dead Sea coast: Geophysical Institute of Israel, Report No 845/319/03.
- Sneh, A., Bartov, Y., Weissbrod, T., and Rosensaft, M., 1998, Geological Map of Israel: Israel Geological Survey, scale 1:200,000, 4 sheets.

Table DR1. Data of the nanoseismic events ($M_L < -1.5$) around the sinkhole cluster of Mineral Beach. The XY location is according to local coordinates and Z is altitude in meters. Seismic velocities are in m/sec.

Date	Time	Station performance					Picking processing					Vp	Vs	X	Y	Z	X_error	Y_error	Z_error	Location	ML	
		st1	st2	st3	st4	st5	st1	st2	st3	st4	st5						m	m	m	error (m)		
03.07.12	5:41:08							PS	PS	PS	750	350	237923.6	606552.9	-441.6	7.3	5.2	69.3	2.6	-2.4		
06.07.12	15:35:42							PS	PS	PS	6200	2000	237807.6	599123.7	-920	10918	7631	113620	2.9	0.4		
17.07.12	23:23:27							PS	PS	PS	750	350	237996.3	606679.7	-438.8	7.5	6.7	106	3.2	-2		
26.07.12	21:05:55						PS	PS	PS		750	350	237923.4	606632.1	-407	3	5.8	54	2.5	-2.5		
27.07.12	20:01:48						PS	PS			PS	2600	600	237791.8	603587.7	-730.7	335	744.8	6957.5	37	-0.9	
27.07.12	20:12:29						PS	PS			PS	720	310	237979.5	606666.5	-400.6	2.1	2.7	38.2	1.9	-2.3	
29.07.12	2:30:42						PS	PS			PS	2600	600	231430.9	611714.5	-2525	1743	1645	1714.8	15.8	-0.2	
29.07.12	13:47:23						PS	PS			PS	720	310	237907.3	606570.5	-443.9	3.5	3.1	27.8	1.4	-2.1	
30.07.12	0:24:03						PS	PS			PS	720	310	237955.9	606295.2	-415.4	6.8	6.9	27.1	12.8	-2.6	
30.07.12	1:23:02						PS	PS			PS	720	310	237876.7	606452.2	-440.6	5.1	4	43.9	10.4	-2.9	
30.07.12	2:19:59						PS	PS			PS	720	310	237865.4	606446.6	-427	279	817.6	100	8.5	-2.5	
01.08.12	12:29:33						PS	PS	PS			720	310	237965.1	606490.5	-406.6	3.9	5.7	30.6	2.9	-2.5	
03.08.12	19:44:44						PS				PS	S	720	310	237926.8	606528.6	-425.5	29.9	4.9	269.7	5.6	-2
04.08.12	9:06:25						PS				PS	PS	750	350	238046	606431.1	-408.5	6.8	11.9	45.3	7.7	-2.4
05.08.12	13:43:48						PS				PS	PS	750	350	237845	606430.7	-425.4	6.7	5.8	48.2	7.4	-2.5
05.08.12	19:44:57						PS				PS	PS	750	350	237890	606579.3	-435	2.4	2	24	0.3	-2.1

05.08.12	20:16:12					S		PS	PS	750	350	237830.5	606569.5	-404.3	11.2	4.3	339.4	2.6	-3.2
05.08.12	20:21:36				PS	PS		PS	PS	750	350	237888.7	606565.6	-428.2	1.5	1.9	16.2	7	-1.7
05.08.12	22:11:04				PS		PS	PS	PS	2000	750	237476.7	605782.1	-506	29.3	66	501.4	8.4	-1.5
06.08.12	2:17:58				PS	PS		PS	PS	750	350	237866.5	606564.5	-424.8	2	2.1	23.1	9.5	-2.3
06.08.12	2:19:36				PS	PS		PS	S	750	350	237875.7	606469.2	-442.8	1.9	2.3	14.2	3.5	-2.6
06.08.12	7:05:37					S		PS	PS	750	350	237877.2	606498.6	-406.3	9.9	5.2	290.9	9.6	-2.8
06.08.12	15:34:04				PS	PS		PS	S	750	350	237867.9	606582.8	-409.5	2.2	2.5	36.4	7.9	-2.2
06.08.12	16:00:13				PS	S		PS	PS	750	350	237834.4	606582.3	-422.7	2.4	1.8	21.4	8.3	-2.8
06.08.12	16:00:18				PS	S		PS	PS	750	350	237829	606436.2	-414.8	3	5.5	58	10.4	-2.5
06.08.12	20:31:26				PS		PS	PS	PS	750	350	237818.4	606592.5	-420.5	3.8	1.9	33.8	2.1	-3.4
07.08.12	2:17:06					S		PS	PS	750	350	237900.5	606788.5	-404.5	13.9	5.4	362	10	-3
07.08.12	21:28:37				PS		PS	PS	PS	750	350	237827.2	606552.5	-404.3	9.5	3.9	291.7	8.4	-3.1
07.08.12	21:38:37				PS	PS		PS	PS	750	350	237893	606558.6	-412.5	1.7	2.5	30	7.9	-2.3
07.08.12	21:49:07					S		PS	PS	750	350	237841.8	606574.8	-435.5	3	2.7	20.6	1.7	-3.6
07.08.12	22:02:33				PS	PS		PS	PS	2000	750	237243.2	606280.5	-605.1	16.5	26.1	66.2	15.3	-0.6
10.08.12	0:54:48				PS		PS	PS	PS	750	350	237863.1	606497.1	-415.9	2.2	3.5	34.5	5.6	-2.4
13.08.12	9:38:42				PS		PS	PS	PS	750	350	237855.5	606259	-442.7	5.5	16	139	8.4	-2.6
13.08.12	5:24:37				S		PS	PS	PS	750	350	237908.8	606733.8	-416.8	4197	671	200	9	-2.7
14.08.12	10:20:22				PS		PS	PS	PS	750	350	238146.1	606384.2	-407	4.4	9	38.6	7.1	-1.8
15.08.12	6:08:45				PS		PS	PS	S	750	350	237819	606383.4	447.8	4.8	9	39.3	0	-3.3

23.08.12	21:17:27						S	S	PS	PS	3500	1500	236187.2	606307	-349.3	575.2	234.6	16975	12.2	-1.1	
23.08.12	23:48:15						S	PS	PS	S	750	350	237694.1	606382.5	-443.1	8.8	11.3	49.4	1	-2.7	
24.08.12	0:43:43						PS	S	S	PS	S	750	350	237773	606335.2	-442.4	7.1	11.6	81.6	2	-2.5
24.08.12	0:44:05						PS	S	S		PS	750	350	237930	606481.9	-422	3	4.7	55.8	4.2	-3.2
24.08.12	2:17:24						PS	S	S	PS	S	750	350	237829.4	606394	-422.4	4.3	8.3	75	3.7	-2.7
24.08.12	2:30:03						PS	S	S	PS	S	750	350	237777.1	606300	-408.9	7.7	7.8	80	4.2	-2.5
24.08.12	2:40:56						PS	S	S	PS	S	750	350	237771.1	606256.1	-429.3	8.2	15.3	165.2	15.3	-2.6
24.08.12	17:19:44						PS	S	S	PS		750	350	237854.7	606361.9	-428.2	5.5	15.5	116.3	4.5	-2.6
24.08.12	3:13:57						PS	S	S	PS	S	750	350	237782.6	606320.2	-440.5	4.9	10.7	83	7.8	-2.3
24.08.12	3:43:46						PS	S	S	PS	S	750	350	237798	606328.6	-431.3	5.4	11.3	101	3.3	-2.6
24.08.12	4:02:01						PS	S	S	PS		750	350	237838.1	606363.1	-441.2	2.8	9	61	5.3	-2.6
24.08.12	4:26:56						PS	PS	S	PS	750	350	238000.9	606750.6	-416	9.6	5.9	225.4	7.7	-3.1	
24.08.12	4:43:35						PS	PS	S	PS	750	350	238007.6	606714.2	-410.2	3.7	3.8	75.3	5.3	-3.2	
24.08.12	7:28:22						PS		PS	PS	PS	750	350	237917.4	606543.4	-415.3	4.3	3.9	69.8	3	-2.2
24.08.12	20:52:45						PS	PS	S	PS	750	350	238011.1	606641.5	-410.8	8.6	4.2	210	6.2	-3.2	
24.08.12	21:30:28						PS	PS	S	PS	750	350	238030.5	606713.4	-411.6	9.9	5	227	6	-3.1	
24.08.12	21:42:30						PS	PS	S	PS	2600	600	238548.1	606336.7	-408	10.2	16.7	240	9.3	-1.1	
24.08.12	23:46:29						PS	PS		PS	750	350	238006.1	606677.3	-411.5	10.8	5.8	256.8	8.4	-2.5	
25.08.12	0:01:24						PS	PS	PS	PS	750	350	237997.3	606635.5	-410.2	8.4	4.1	210	3.1	-3.4	
25.08.12	0:03:50						PS	PS	PS	PS	750	350	238011.7	606678.3	-411.9	8.7	4.2	214.4	8.1	-3	

25.08.12	0:07:12							PS	PS	PS	PS	750	350	238009.1	606699.5	-410.2	8.1	3.9	185.6	6	-3
25.08.12	0:09:07							PS	PS	PS	PS	750	350	237991.4	606624.9	-410.5	7.1	3.6	183	4.1	-2.6
25.08.12	0:25:47							PS	PS		PS	2600	750	238418.1	606713.4	-405.1	7.9	16	165.4	9.4	-2.1
25.08.12	0:26:04						P	S	S	PS	PS	750	350	237758.2	606395.3	-420.7	5.5	8.5	74.5	14.4	-2.2
25.08.12	0:29:12						PS	S	PS	PS	PS	750	350	237754.4	606388.4	-419.9	4.7	7.4	67.2	6.8	-2.4
25.08.12	0:36:03						PS	PS			PS	750	350	238042.7	606650.3	-412.7	9.9	5.1	238	5.8	-2.9
25.08.12	0:37:15						PS	PS		S	PS	2600	600	239268.7	606774.4	-473.3	237.6	161.4	5281	24	-1.1
25.08.12	0:37:47						S	PS	PS	PS	PS	750	350	237975.6	606744.2	-422.7	2.5	3.5	50.3	8.3	-2.2
25.08.12	0:37:57						S	PS	PS	PS	PS	750	350	238048.4	606724.4	-429	2.3	3.5	38.6	10.8	-2.2
25.08.12	6:16:47						PS	S	S	PS	S	750	350	237802	606406.1	-416.8	5	8.2	75.7	4.3	-2.9
02.09.12	9:55:49						PS	PS	PS	PS	PS	750	350	238006.4	606690.8	-409.8	7.5	3.7	171	7.7	-2.4
03.09.12	3:13:37						PS	PS	PS	PS	PS	750	350	237982.9	606693.7	-411	8	3.9	204	1.1	-3.1
03.09.12	7:13:17						PS	PS	PS	PS	PS	750	350	237943.5	606624.7	-411.8	5.5	3.5	145	7.3	-3.1
04.09.12	0:28:23						PS	PS	PS	PS	PS	750	350	237964.1	606704.5	-413.5	5.8	3.9	128.9	3.2	-2.5
04.09.12	0:30:54						PS	PS	PS	PS	PS	750	350	237974.7	606705.8	-413.9	6	4.1	136.3	6.5	-2.9
04.09.12	11:50:27						S	PS	PS	PS	PS	750	350	237837	606600.5	-404	7	3.2	208	4.1	-3
05.09.12	1:57:02						S	PS		PS	PS	750	350	237899.3	607017.3	-413	895.4	378.9	18761	5.9	-3
05.09.12	1:57:35						S	PS		PS	PS	750	350	237901.2	606723.8	-407.5	1884.8	850	38938	9.3	-2.8
05.09.12	2:15:28						PS	S		PS	PS	750	350	237744	606615.6	-421.5	8	16.6	120	6.6	-2.9
05.09.12	2:15:40						PS	S		PS	PS	750	350	237837.6	606673.2	-429	5.7	11.6	36.3	1.7	-2.6

05.09.12	19:56:28						PS	PS		PS	750	350	237945.7	606774.5	-447.7	4.5	8.7	34.6	2.7	-2.6
05.09.12	20:33:07						PS	PS		PS	750	350	237751.5	606507.2	-447.6	6.4	14.9	76.6	1.8	-2.3
05.09.12	20:36:08						PS	S		PS	750	350	237739.1	606569.1	-430.9	7.9	17.2	117.5	2.2	-2.7
07.09.12	0:42:01						PS	PS		PS	750	350	237987.2	606692.8	-435	2.4	4.6	37.8	2.1	-3.2
07.09.12	10:54:18						S	PS		PS	750	350	237902.5	606750.6	-445.4	6.2	11.2	40.9	1.8	-2.7
07.09.12	22:44:08						PS	PS	S	PS	750	350	237849.6	606417.2	-421.7	3.9	9.1	79.3	5.6	-2.4